Strong exciton-photon coupling in inorganic-organic multiple quantum wells embedded low-Q microcavity

K. Pradeesh[1], J. J. Baumberg[2] and G. Vijaya Prakash[1]*

[1]*Nanophotonics lab, Department of Physics, Indian Institute of Technology Delhi, New Delhi-110016, India*
[2]*Nanophotonics Centre, Cavendish Laboratory, University of Cambridge, Cambridge, CB3 0HE, United Kingdom*
*prakash@physics.iitd.ac.in

Abstract: Optoelectronic-compatible heterostructures are fabricated from layered inorganic-organic multiple quantum wells (IO-MQW) of Cyclohexenyl ethyl ammonium lead iodide, $(C_6H_9C_2H_4NH_3)_2PbI_4$ (CHPI). These hybrids possess strongly-resonant optical features, are thermally stable and compatible with hybrid photonics assembly. Room-temperature strong-coupling is observed when these hybrids are straightforwardly embedded in metal-air (M-A) and metal-metal (M-M) low-Q microcavities, due to the large oscillator strength of these IO-MQWs. The strength of the Rabi splitting is 130meV for M-A and 160meV for M-M cavities. These values are significantly higher than for *J*-aggregates in all-metal microcavities of similar length. These experimental results are in good agreement with transfer matrix simulations based on resonant excitons. Incorporating exciton-switching hybrids allows active control of the strong-coupling parameters by temperature, suggesting new device applications.

OCIS codes: (160.4670) Optical materials; (250.5230) Photoluminescence; (250.4745) Optical processing devices; (140.3948) Microcavity devices; (310.3840) Materials and process characterization

References and links

1. S. Noda, M. Fujita, and T. Asano, "Spontaneous-emission control by photonic crystals and nanocavities," Nat. Photonics **1**(8), 449–458 (2007).
2. A. Ródenas, G. Zhou, D. Jaque, and M. Gu, "Rare-Earth Spontaneous Emission Control in Three-Dimensional Lithium Niobate Photonic Crystals," Adv. Mater. **21**(34), 3526 (2009).
3. M. Li, A. Xia, J. Wang, Y. Song, and L. Jiang, "Coherent control of spontaneous emission by photonic crystals," Chem. Phys. Lett. **444**(4-6), 287–291 (2007).
4. P. V. Kelkar, V. G. Kozlov, and A. V. Nurmikko, C. C. Chu, J. Han and R. L. Gunshor, "Stimulated emission, gain, and coherent oscillations in II-VI semiconductor microcavities," Phys. Rev. B **56**(12), 7564–7573 (1997).
5. V. Bulović, V. B. Khalfin, G. Gu, P. E. Burrows, and S. R. Forrest, "Weak microcavity effects in organic light-emitting devices," Phys. Rev. B **58**(7), 3730–3740 (1998).
6. R. B. Fletcher, D. G. Lidzey, D. D. C. Bradley, M. Bernius, and S. Walker, "Spectral properties of resonant-cavity, polyfluorene light-emitting diodes," Appl. Phys. Lett. **77**(9), 1262 (2000).
7. C. Weisbuch, M. Nishioka, A. Ashikawa, and Y. Arakawa, "Observation of the coupled exciton-photon mode splitting in a semiconductor quantum microcavity," Phys. Rev. Lett. **69**(23), 3314–3317 (1992).
8. D. G. Lidzey, D. D. Bradley, M. S. Skolnick, T. Virgili, S. Walker, and D. M. Whittaker, "Strong exciton-photon coupling in an organic semiconductor microcavity," Nature **395**(6697), 53–55 (1998).
9. P. G. Savvidis, J. J. Baumberg, R. M. Stevenson, M. S. Skolnick, D. M. Whittaker, and J. S. Roberts, "Angle-Resonant Stimulated Polariton Amplifier," Phys. Rev. Lett. **84**(7), 1547–1550 (2000).
10. M. Vladimirova, S. Cronenberger, D. Scalbert, M. Nawrocki, A. V. Kavokin, A. Miard, A. Lemaître, and J. Bloch, "Polarization controlled nonlinear transmission of light through semiconductor microcavities," Phys. Rev. B **79**(11), 115325 (2009).
11. S. Christopoulos, G. B. von Högersthal, A. J. D. Grundy, P. G. Lagoudakis, A. V. Kavokin, J. J. Baumberg, G. Christmann, R. Butté, E. Feltin, J. F. Carlin, and N. Grandjean, "Room-Temperature Polariton Lasing in Semiconductor Microcavities," Phys. Rev. Lett. **98**(12), 126405 (2007).

#115949 - $15.00 USD Received 19 Aug 2009; revised 23 Sep 2009; accepted 27 Sep 2009; published 19 Nov 2009

12. J. P. Reithmaier, G. Sek, A. Löffler, C. Hofmann, S. Kuhn, S. Reitzenstein, L. V. Keldysh, V. D. Kulakovskii, T. L. Reinecke, and A. Forchel, "Strong coupling in a single quantum dot-semiconductor microcavity system," Nature **432**(7014), 197–200 (2004).
13. P. G. Lagoudakis, M. D. Martin, J. J. Baumberg, A. Qarry, E. Cohen, and L. N. Pfeiffer, "Electron-Polariton Scattering in Semiconductor Microcavities," Phys. Rev. Lett. **90**(20), 206401 (2003).
14. D. G. Lidzey, A. M. Fox, M. D. Rahn, M. S. Skolnick, and S. Walker, "Experimental study of light emission from strongly coupled organic semiconductor microcavities following nonresonant laser excitation," Phys. Rev. B **65**(19), 195312 (2002).
15. S. Kéna-Cohen, M. Davanço, and S. R. Forrest, "Strong Exciton-Photon Coupling in an Organic Single Crystal Microcavity," Phys. Rev. Lett. **101**(11), 116401 (2008).
16. C. E. Finlayson, G. V. Prakash, and J. J. Baumberg, "Strong exciton-photon coupling in a length tunable optical microcavity with J-aggregate dye heterostructures," Appl. Phys. Lett. **86**(4), 041110 (2005).
17. M. Era, S. Morimoto, T. Tsutsui, and S. Saito, "Organic–Inorganic Heterostructure Electroluminescent Device Using a Layered Perovskite Semiconductor $(C_6H_5C_2H_4NH_3)_2PbI_4$," Appl. Phys. Lett. **65**(6), 676 (1994).
18. C. R. Kagan, D. B. Mitzi, and C. D. Dimitrakopoulos, "Organic-Inorganic Hybrid Materials as Semiconducting Channels in Thin-Film Field-Effect Transistors," Science **286**(5441), 945–947 (1999).
19. T. Dantas de Morais, F. Chaput, K. Lahlil, and J. P. Boilot, "Hybrid Organic–Inorganic Light-Emitting Diodes," Adv. Mater. **11**(2), 107–112 (1999).
20. G. V. Prakash, K. Pradeesh, R. Ratnani, K. Saraswat, M. E. Light, and J. J. Baumberg, J. Phys: D App. Phys. **42**, 185405 (2009).
21. S. Zhang, G. Lanty, J.-S. Lauret, E. Deleporte, P. Audebert, and L. Galmiche, "Synthesis and optical properties of novel organic–inorganic hybrid nanolayer structure semiconductors," Acta Mater. **57**(11), 3301–3309 (2009).
22. K. Pradeesh, J. J. Baumberg, and G. V. Prakash, "In situ intercalation strategies for device-quality hybrid inorganic-organic self-assembled quantum wells," Appl. Phys. Lett. **95**(3), 033309–033311 (2009).
23. T. Ishihara, J. Takahashi, and T. Goto, "Optical properties due to electronic transitions in two-dimensional semiconductors (C_nH_2n+1NH_3)_2PbI_4," Phys. Rev. B **42**(17), 11099–11107 (1990).
24. P. A. Hobson, W. L. Barnes, D. G. Lidzey, G. A. Gehring, D. M. Whittaker, M. S. Skolnick, and S. Walker, "Strong exciton–photon coupling in a low-Q all-metal mirror microcavity," Appl. Phys. Lett. **81**(19), 3519 (2002).
25. G. Lanty, A. Bréhier, R. Parashkov, J. S. Lauret, and E. Deleporte, "Strong exciton–photon coupling at room temperature in microcavities containing two-dimensional layered perovskite compounds," N. J. Phys. **10**(6), 065007 (2008).
26. K. Sumioka, H. Nagahama, and T. Tsutsui, "Strong coupling of exciton and photon modes in photonic crystal infiltrated with organic–inorganic layered perovskite," Appl. Phys. Lett. **78**(10), 1328–1330 (2001).
27. D. G. Billing, and A. Lemmerer, "Synthesis, characterization and phase transitions of the inorganic–organic layered perovskite-type hybrids $[(C_nH_{2n+1}NH_3)_2PbI_4]$ (n = 12, 14, 16 and 18)," N. J. Chem. **32**(10), 1736–1746 (2008).
28. K. Pradeesh, J. J. Baumberg, and G. V. Prakash, "Exciton Switching and Peierls Transitions in Hybrid Inorganic-Organic Self-Assembled Quantum Wells", Communicated (2009).

1. Introduction

Achieving better control of the spontaneous emission in optoelectronic devices has been a major focus of research in photonics structures, particularly using microcavities [1–4]. Confining emitters within microcavities modifies their emission in two related regimes; weak coupling and strong coupling. In weak coupling, the spatial and the temporal distribution of the emitted radiation is modified and hence the spontaneous emission is enhanced or suppressed, which is of use in applications such as vertical cavity surface emitting lasers and resonant cavity light emitting diodes [5, 6]. In contrast for larger light-matter coupling, if exciton and photon lifetimes are long in comparison to their interaction time, they mix in a strong coupling regime in which new coupled eigenstates called polaritons emerge [7, 8]. In this regime, the microcavity polariton dispersion $E(k)$ consists of anti-crossing branches separated in energy by the Rabi splitting, Ω, which defines the coupling strength. This situation has been of intense interest due to the coherent and stimulated optical effects elicited which can lead to new optical devices [9–11]. Although exciton-photon coupling in such strong-coupling cavities is of great interest, most studies focus on using inorganic emitters (semiconductor Quantum Dots (QDs) and Quantum Wells) in high Q-factor planar microcavities at low temperatures [12,13]. Organic semiconductors are most promising alternatives as laser media and strong *Frenkel* exciton-photon coupling has now been realized even at room temperatures [8, 14, 15]. Recently we reported strong coupling in *low Q*-microcavities containing 50nm organic layers (of *J*-aggregates) [16]. However, trivial problems related to organic semiconductors, such as low-melting values, device-compatible processing issues, and photo-oxidation are limiting factors for practical applications. Recent

#115949 - $15.00 USD Received 19 Aug 2009; revised 23 Sep 2009; accepted 27 Sep 2009; published 19 Nov 2009

progress in the structural engineering of 'naturally' self-assembled 2D layered inorganic-organic multiple quantum wells (IO-MQW) show new possibilities for optoelectronics devices with tremendous advantage over the conventional organics [17–19]. These metal-halide-based IO-MQWs are thermally stable up to 200°C [20], and a wide range of structures can be conveniently synthesized by choosing an appropriate intercalating organic moiety [21]. While fabrication of well-ordered thin films is not always straightforward, we recently reported a simple intercalation strategy, compatible with fabrication of photonic devices, to yield well-ordered films over cm^2-scale areas [22].

Here we fabricate large area heterostructures from a self-assembled hybrid quantum well, 2-(1-Cyclohexenyl) ethyl ammonium lead iodide, $(C_6H_9C_2H_4NH_3)_2PbI_4$ (hereafter CHPI). We show the ability of these hybrids to generate the strong coupling regime even at room temperatures in low-Q factor microcavities. We further demonstrate the tunability in these strongly-coupled microcavities by using a similar hybrid, C12PI, which allows switchable excitons.

2. Experiment

Thin films and single crystals of 2-(1-Cyclohexenyl) ethyl ammonium lead iodide, $(C_6H_9C_2H_4NH_3)_2PbI_4$ (CHPI) were prepared by both intercalation and chemical synthesis described previously [20, 22]. Briefly, the chemical synthesis was carried out by taking stoichiometric amounts of PbI_2 and 2-(1-cyclohexenyl) ethyl amine ($C_6H_9C_2H_4NH_2$) [see 20]. The resulting orange precipitate was filtered, dried and used to harvest single crystals of dimensions 2x2x.0.5mm^3 from methanolic solution by slow evaporation. X-Ray diffraction confirms the natural self assembly of layered films. Microcavities were fabricated as follows: firstly silver (48nm) is sputtered onto a clean glass substrate, followed by sputtering of a SiO_2 layer (335nm) on top of the Ag. Subsequently PbI_2 (~72nm) was coated onto this structure and subsequently processed to obtain CHPI through intercalation, as described earlier [22]. This forms a metal-insulator-CHPI-air (M-A) microcavity. For metal-hybrid-metal (M-M) cavities, a layer of poly(methyl methacrylate) (PMMA) polymer (125nm) was spun on top of the CHPI and subsequently a partially-reflecting Ag mirror of thickness ~10nm was coated by thermal vapor deposition. Similar methods of synthesis and fabrication were followed for the C12PI-based microcavity. PL and transmission imaging/spectroscopy used a modified laser scanning confocal microscope fitted with a diode laser (447nm), white light source and a spectrometer.

3. Results and discussion

In these hybrid 2D layered networks, inorganic semiconductor and organic layers are stacked alternatively. These are regarded as *natural multiple quantum well* (MQW) structures [23], with ~6Å semiconductor layers as '*well'* material and wider-bandgap ~10Å organic layers as the '*barrier'* [Fig. 1(A)]. Strong room-temperature excitons in these heterostructures arise due to the low dimensionality of the inorganic structure (quantum confinement), as well as large dielectric mismatch (dielectric confinement) between the organic and inorganic layers [23]. Films processed using the intercalation strategy show narrow X-ray diffraction peaks [Fig. 1(B)] corresponding to the (001) plane at 2θ=5°, followed by higher diffraction orders related to (00l) (l=2, 3, 4,…) thus confirming that the CHPI films are highly self-organized into layers and perfectly orientated on the substrate. Such films show room-temperature high-oscillator-strength excitonic absorption at ~510nm and strong photoluminescence (PL) at ~523nm [Fig. 1(C)]. Both absorption and PL show symmetric narrow lineshapes with FWHM less than 20nm.

#115949 - $15.00 USD Received 19 Aug 2009; revised 23 Sep 2009; accepted 27 Sep 2009; published 19 Nov 2009

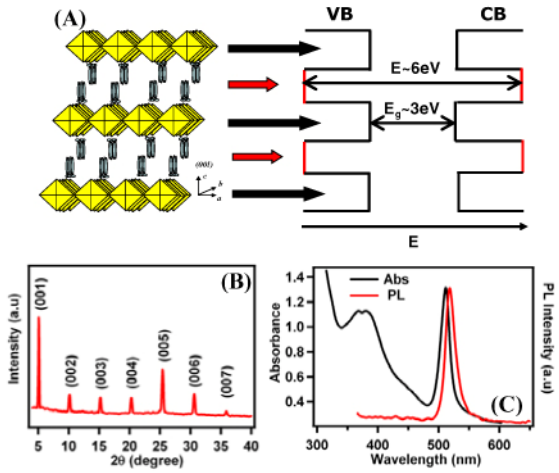

Fig. 1. (A) Schematic diagram of CHPI layered structure with the corresponding energy level diagram showing the band gap of organic and inorganic layers. (B) X-ray diffraction pattern of CHPI thin film. (C) UV-Visible absorption and PL features of CHPI thin film.

It is essential to examine the nature and morphology of the CHPI thin films prior to their integration into microcavities, since its PL characteristics are strongly dependent on structural re-arrangement of layers. Figure 2 gives the morphological study through transmission and PL intensity mapping of a micron sized single crystal. The confocal microscopic image, PL image and laser scattered image of the crystal under study are shown in Figs. 2(A), (B) and (C) respectively. As the thickness of the crystal is in the order of microns the transmission image is totally saturated at the peak exciton absorption wavelength 510nm [Fig. 2(D)]. As seen from Fig. 2(E), PL mapping of the single crystal shows strong and narrow exciton PL peak at 523nm, uniformly throughout the crystal. However, a broad shoulder at about 545nm has also been observed at the crystal edges. The uneven packing of layer stacking at the edges of the crystal may result into more crystal defects, thus the defect related broad emission at 545nm [20].

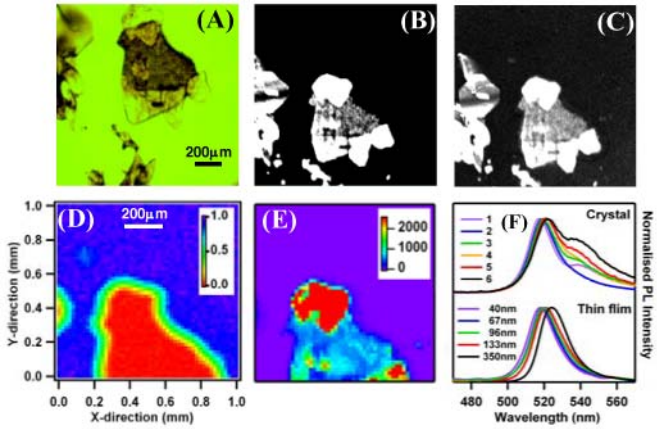

Fig. 2. (A) Confocal transmission image (B) PL image with 510nm high pass filter and (C) Laser (447nm) scattered image of CHPI single crystal. (D) and (E) Transmission and PL intensity spatial scans of the crystal at selective wavelengths 510nm and 523nm respectively. (F) PL spectra of CHPI thin films with different thicknesses and PL of single crystal at different positions (in mm) (0.34, 0.38), (0.46, 0.30), (0.34, 0.30), (0.40, 0), (0.34, 0.06) and (0.20, 0.30) respectively for labels 1 to 6.

In contrast to measurements on the single crystals, in thin films the PL mapping (not shown here) is spatially uniform and no such defect-related emission has been observed.

#115949 - $15.00 USD Received 19 Aug 2009; revised 23 Sep 2009; accepted 27 Sep 2009; published 19 Nov 2009

However, a peculiar feature still under investigation is the PL red-shift (~10nm) [Fig. 2(F)] when the thickness is increased from 40nm to 350nm. We believe this arises either due to distorted bond angles within the lead iodide layered network or due to the presence of unreacted lead iodide impurities [22]. From these mapping measurements, it is clear that sub-100nm thick films of CHPI are optimal to produce the strong coupling regime.

Having optimized the fabrication strategy for uniform thin CHPI films they are placed within low-Q microcavities. The first M-A cavity is designed as a 5λ/4 thick cavity, with Ag/SiO_2 (R=86%) and CHPI/air as high and low reflecting ends [Fig. 3(A)]. The SiO_2 spacer thickness is adjusted so that the cavity mode is in resonance with the exciton state. Angle-resolved transmission spectra of the M-A cavity are recorded using TE-polarized white light [Fig. 3(B)]. The photonic mode at 2.3eV (540nm) of width ~0.12eV (~70nm) splits into two branches at the exciton transmission dip around 2.45eV (523nm), at an incident angle of 33°. To confirm this, full-transfer-matrix simulations [16], are performed using the experimentally-extracted optical constants (n and k) of CHPI from white-light ellipsometry, and the values reported in literature for Ag and SiO_2 over the wide region of wavelengths, λ=300-800nm [Fig. 3(C)]. Both simulated and experimental transmission spectra clearly reveal characteristic anti-crossing transmission dips from strong-coupling of the excitonic and cavity modes forming two new branches, lower polariton (LP) and upper polariton (UP) branches. A spatial map of the optical intensity inside the microcavity as a function of incident angle clearly shows the resonant enhancement at 33° [Fig. 3(E)]. Similarly a spatial map of the intensity inside the microcavity at different incident energies shows the two polariton modes [Fig. 3(D)], which in this situation do not overlap strongly with the CHPI layer. Despite this, the vacuum Rabi splitting defined by the minimum energy separation between the LPB and UPB is 130meV. This anti-crossing is a clean signature of strong coupling between CHPI hybrid exciton and the cavity photonic mode.

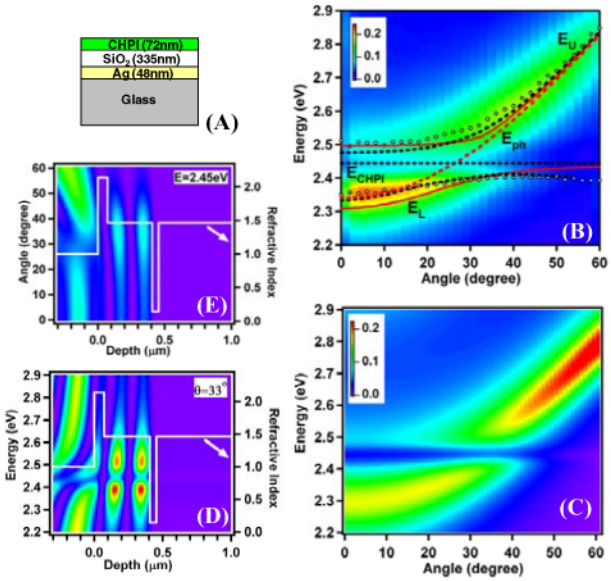

Fig. 3. (A) Metal-air microcavity. (B) Experimental angle-dependent transmission spectral image, solid circles are transmission dip minima. Transfer-matrix (red line) and two-level model (black dashed) also shown. (C-E) Transfer-matrix simulations of (C) angle-dependent transmission spectral image, (D) spatial map of optical intensity *vs* photon energy at 33° and (E) spatial map of optical intensity *vs* angle at energy 2.45eV

The dispersion relations of the polaritonic branches also match the standard two-level model [16] with UP (E_U) and LP (E_L) defined by Eq. (1)

#115949 - $15.00 USD Received 19 Aug 2009; revised 23 Sep 2009; accepted 27 Sep 2009; published 19 Nov 2009

$$E_{U,L}(\theta)=\frac{\left[E_{ph}(\theta)+E_{CHPI}\right]}{2}\pm\sqrt{\frac{\Omega^2}{4}+\frac{\left[E_{ph}(\theta)-E_{CHPI}\right]^2}{4}} \quad (1)$$

where E_{CHPI} and $E_{ph}(\theta)$ are the energies of CHPI excitonic state and the bare cavity photon mode respectively. The cavity photonic mode $E_{ph}(\theta)$ is related to the transmission angle, as $E_{ph}(\theta)=E_c\left(\sqrt{1-\sin^2\theta/n_{eff}^2}\right)^{-1}$, where the fitting parameters E_c and n_{eff} are the cavity photon energy at normal incidence and effective cavity refractive index, respectively. The values thus obtained for M-A cavity are E_c=2.34eV n_{eff} =1.54. Relatively low effective refractive index confirms that most of the optical field is in the SiO_2 layers, with the modes [Fig. 3(B)] matching well the transfer simulations.

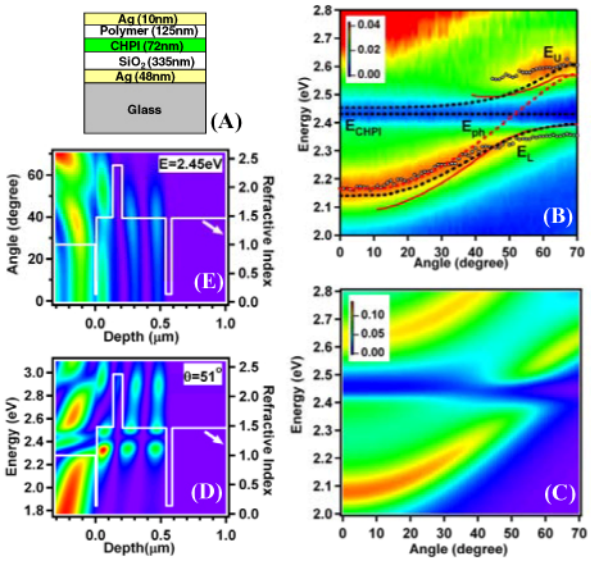

Fig. 4. (A) Schematic diagram of the M-M microcavity. (B) Experimental angle-dependent transmission spectral image. Solid circles are from experimental transmission dips. Solid (red) and dashed (black) lines are from transfer-matrix and two-level mode simulations respectively (see text). Transfer-matrix simulated (C) angle-dependent transmission spectral image, (D) spatial map of optical intensity vs energy at 51° and (E) spatial map of optical intensity vs angle at energy 2.45eV.

Similar results are found for all-metallic (M-M) microcavities of optical length 7λ/4. Here an additional 125nm buffer layer of polymer (PMMA) is spin-coated on the M-A cavity, and a final deposition of 10nm Ag (R=35%) completes the microcavity [Fig. 4(A)]. Once again angle-resolved transmission spectra, shown in Fig. 4(B), match the transfer matrix simulations in Fig. 4(C). The fitting parameters from two-level model for M-A cavity are E_c=2.15eV and n_{eff}=1.69. The spatial map of optical intensity vs energy at the anti-crossing angle (51°) and optical intensity vs angle at the CHPI exciton energy (2.45eV) are shown in Fig. 4 (D) and (E). The M-M cavity produces a more prominent anti-crossing, with a Rabi splitting of 160meV at an angle of 51° due to the greater field confinement. The penetration of the optical field in the CHPI in the present cavity results into comparatively higher n_{eff} than the open M-A cavity (n_{eff}=1.54). These Rabi splitting values of both M-A and M-M cavities are much larger than that of previously reported all-metallic organic (J-aggregate) microcavities [16,24], and comparable to hybrid microcavities of similar cavity lengths [25, 26].

#115949 - $15.00 USD Received 19 Aug 2009; revised 23 Sep 2009; accepted 27 Sep 2009; published 19 Nov 2009

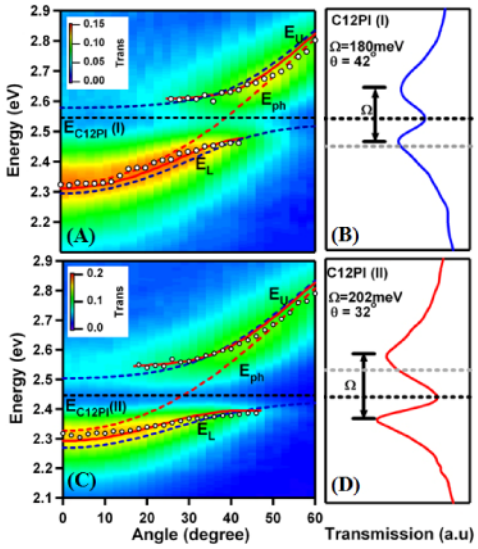

Fig. 5. (A) and (C) are experimental angle-dependent transmission spectral images of M-A cavity with C12PI excitons of aged (Phase I) and fresh (Phase II) cavities respectively (see text). Solid circles are from experimental transmission dips. Solid (red) and dashed (blue) lines are from transfer-matrix and two-level mode simulations respectively. (B) & (D) Transmission spectra of the M-A cavity of the Phase (I) and Phase (II) excitons respectively at the anti-crossing angles.

The opportunities afforded by hybrid inorganic-organic quantum wells is exemplified by creating microcavities [Fig. 5] in which the Rabi frequency can be switched in situ. We demonstrate this tunability in strong coupling by replacing the hybrid CHPI with a phase-changing hybrid known as C12PI [27], in M-A cavity of Fig. 3. This C12PI hybrid exhibits a clear shift in exciton energy (from 2.53eV to 2.44eV) when it undergoes a layer-'crumpling' structural phase transition from C12PI(I) to C12PI(II), due to temperature (T_c=60°C) and/or aging. These structural flips show completely reversible thermal hysteresis and also thickness dependent. Therefore, it is possible to switch the optical features between these two phases by controlling the thickness and/or the temperature. Also, this phase transformation can be prevented by annealing the films at 60°C for an hour or by overcoating the film with a protective layer such as polymer. While a detailed discussion of this rapid Peierls-switching and the resulting exciton response will be published elsewhere [28], the digital flip of exciton energy provides a reversible way to control microcavities. Angle-dependent transmission spectra [Fig. 5(C)] of a freshly-deposited C12PI (II) M-A cavity is seen to flip when transformed to C12PI(I) [Fig. 5(A)], in this case by ageing for 1 day, under ambient conditions. While strong-coupling in the C12PI(I) M-A cavity gives a Rabi splitting of 180meV at 42° [Fig. 5(B)], the C12PI(II) cavity exhibits increased Rabi splitting of 202meV at 32° [Fig. 5(D)]. Hence both the strong-coupling angle and coupling rate vary by flipping the constituent phase. These PbI_4 (sheet-crumpling) phase changes of C12PI are controllable and completely reversible. Therefore our experiments demonstrate the general ability of inorganic-organic hybrids even in low Q cavities for strong coupling.

4. Conclusions

Here we fabricated and studied layered perovskite inorganic-organic multiple quantum well heterostructures of CHPI. These narrow-exciton-linewidth hybrids show little Stokes shift between emission and absorption peaks, and are thus highly suited for strong-coupling applications. Incorporating such hybrid thin films in M-A and M-M low-Q cavities provides clear room-temperature strong coupling phenomena. The Rabi splitting is found to be ~130meV for M-A and ~160meV for M-M low-Q microcavities respectively, with

#115949 - $15.00 USD Received 19 Aug 2009; revised 23 Sep 2009; accepted 27 Sep 2009; published 19 Nov 2009

controllable *in situ* switching between 180meV and 202meV in comparable C12PI microcavities. Strong coupling of these IO-MQWs paves the way for new device applications, particularly optimal for polariton laser experiments, since these films are more robust in nonlinear experiments than comparable organics. Further, these hybrids are of significance in fabricating robust optoelectronic devices.

Acknowledgements

Authors are thankful to Department of Science & Technology (DST), India for the financial support. This work is part of UK-India Education Research Initiative (UKIERI), and part funded by EPSRC grant EP/C511786/1.

#115949 - $15.00 USD Received 19 Aug 2009; revised 23 Sep 2009; accepted 27 Sep 2009; published 19 Nov 2009